500 ppm, respectively) revealed treatment-related effects on the levels of spontaneously occurring mammary tumors. The number of benign mammary tumors per tumor-bearing rat was increased in each of these studies (Burek *et al.*, 1984). This observation is consistent with the observation of increased benign mammary tumors in a similar inhalation study (up to 4000 ppm) in the F344 rat (NTP, 1985). Low incidences of tumors in the ventral neck region in and around the salivary gland of male rats were noted in one study (Burek *et al.*, 1984) but were not noted in the other two rat inhalation studies (Burek *et al.*, 1984; NTP, 1985).

Significant increases in spontaneously occurring lung and liver tumors were noted when B6C3F1 mice were exposed to 2000 or 4000 ppm of DCM. In contrast to the studies mentioned above, where DCM either failed to affect the tumor incidence or affected primarily benign tumors, the incidence of both benign and malignant tumors was elevated in this study (NTP, 1985).

The obvious question raised by these new findings is whether humans exposed to DCM are likely to develop tumors similar to those seen in mice. While there are many biological factors which must be considered in answering this question, one of the primary considerations involves differences in delivery of toxic chemicals to target tissues in the various species.

Conventional risk assessments have typically involved linear extrapolation of external dose, combined with an interspecies factor based on body surface area. By contrast, pharmacokinetic models permit the calculation of internal doses through integration of information on the administered dose, the physiological structure of the mammalian species, and the biochemical properties of the specific chemicals. Predicted internal doses can be correlated with toxicity and/or tumor incidence to yield hypotheses of the mechanisms of action of particular chemicals. Clewell and Andersen (1985) have previously discussed the reasons why the scientific basis (soundness) of the risk assessment process could be improved through the use of physiologically based pharmacokinetic (PB-PK) modeling.

To apply these principles to a DCM risk assessment, we constructed a PB-PK model of DCM disposition. This model provided quantitative descriptions of the rates of metabolism and levels of DCM in various organs of four mammalian species (rats, mice, hamsters, and humans). The PB-PK model was validated with blood concentration/time-course data from rats, mice, and humans exposed to DCM. Next, model output parameters were correlated with the tumor incidences in two chronic bioassays of DCM in the B6C3F1 mouse (NTP, 1985; Serota *et al.*, 1984a) to formulate a hypothesis for the mechanism of tumorigenicity. Finally, relevant measures of tissue dose were calculated for use in a pharmacokinetically based risk assessment process.

METHODS

Model structure. Ramsey and Andersen (1984) described a general PB-PK model for inhalation of volatile metabolized chemicals. This general model was modified for use with DCM (Fig. 1). Since DCM caused both liver and lung tumors, the PB-PK model developed had to include both of these tissues. Consequently this model differed from that of Ramsey and Andersen (1984) by having a distinct, metabolically active lung compartment which was placed between the gas exchange compartment and systemic arterial blood (Fig. 1).

Transport of DCM between alveolar air and blood occurs in the gas exchange compartment in the model. Because equilibration of air with the blood in the lung occurs rapidly, it was assumed that gas/blood exchange was completed before DCM entered the lung tissue compartment. In drinking water simulations, DCM was absorbed by a zero-order process, entering the liver compartment at a constant hourly rate (mg/hr) equal to 1/24 the daily dose. This assumes 100% absorption of the ingested dose and is consistent with results obtained with other halogenated hydrocarbons administered in the drinking water (tetrachloroethylene, Frantz and Watanabe, 1983; methylchloroform, Reitz *et al.*, 1986, unpublished data). Intravenous administration was simulated as a very short

(0.01–0.03 hr) infusion of DCM directly into mixed venous blood.

Pulsatile drinking scenarios could also have been used to describe the drinking water input function. In a recent publication (National Research Council, 1986) total daily ingestion of volatile organic compounds in drinking water was described by a number of episodic inputs evenly spaced over half the day. The numbers of daily inputs examined were 72, 12, 6, and 1, the last value corresponding to bolus intubation. Only very minor differences in pharmacokinetic behavior were noted when the number of inputs was increased from 12 to 72. Zero-order input is equivalent to a very large number of pulsatile inputs and would be expected to behave very similarly to the 12- or 72-input scenarios.

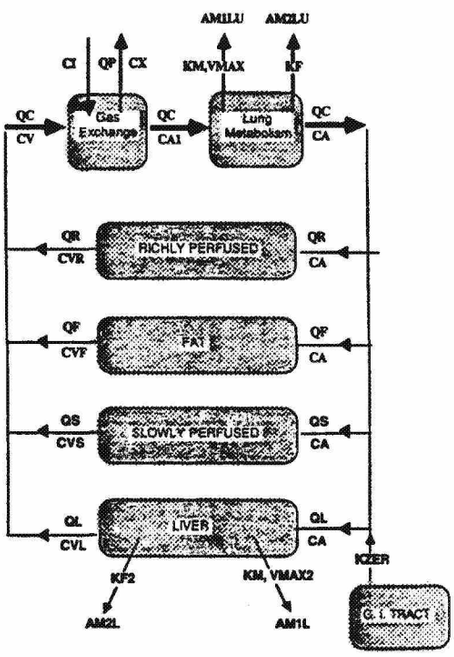

FIG. 1. Diagram of the physiologically based pharmacokinetic model utilized for methylene chloride (dichloromethane, DCM). This model is an adaptation of one reported previously by Ramsey and Andersen (1984) for describing the metabolism of styrene. Tissues of the body are grouped into five compartments with similar flow and partition coefficients: Lung, fat, liver, richly perfused, and slowly perfused. Metabolism occurs in the lung and liver compartments. DCM enters the body through inhalation with absorption into pulmonary blood in the gas exchange compartment, or by ingestion with absorption directly into the liver compartment. Details of the model may be found in the Appendices to this paper.

Mass balance differential equations for the model were similar to those of Ramsey and Andersen (1984) except for liver and lung tissue. Definitions of the algebraic constants and differential equations used for lung and liver tissue may be found in Appendix A.

Most of the simulations conducted with this model were also conducted with an alternate model in which the processes in the lung were described as occurring in a single compartment. The two formulations gave essentially equivalent results for the cases examined in this paper. The former model was chosen for computational simplicity.

Model parameters. To implement this physiological analysis three major types of data are required: (1) partition coefficients (expressing the relative solubility of DCM in various tissues), (2) physiological constants (for blood flows and tissue volumes), and (3) biochemical constants (for important biotransformation pathways). These constants were obtained by experimentation or from the literature for each species of interest: mouse, rat, hamster, and human.

Partition coefficients. Partition coefficients were determined with a vial equilibration technique (Sato and Nakajima, 1979) in which DCM was added to a closed vial containing test liquid. Partitioning was determined by measuring the concentration of DCM in the head space after 1 or 2 hr of incubation at 37°C.

Blood/air partition coefficients were measured in samples of rat, mouse, hamster, and human blood. Tissue/air partition coefficients for liver, muscle, and fat were determined in tissues from the rat and hamster. Partition coefficients for the richly perfused nonmetabolizing tissue group and lung tissue were assumed to be equal to the measured liver/air partition coefficient. Partition coefficients for the slowly perfused tissue group were assumed to be equal to the measured muscle/air partition coefficient. Tissue/air partition coefficients for mouse and human tissue were not determined and were assumed to be equal to those measured in the rat. Tissue/blood partition coefficients were calculated by dividing the tissue/air coefficients for each tissue by the blood/air partition coefficient for that species. All partition coefficient determinations were carried out in one of our laboratories (Wright–Patterson AFB), and the values employed in the model are listed in Table 1.

Physiological constants. Volumes of tissue and blood flows to the various tissue groups (Table 1) were taken from the literature (ICRP, 1975; Davis and Mapleson, 1981; Caster *et al.*, 1956) and are consistent with values used in other physiological descriptions of the pharmacokinetics of xenobiotics (Ramsey and Andersen, 1984; Gargas *et al.*, 1986a; Fiserova-Bergerova, 1975). The lung weight is proportional to body weight (Leith, 1976)

TABLE 1

KINETIC CONSTANTS AND MODEL PARAMETERS USED IN THE PHYSIOLOGICALLY BASED PHARMACOKINETIC MODEL FOR DICHLOROMETHANE

	B6C3F1[a]	F344 rats[b]	Hamsters[b]	Human
Weights (kg)				
Body	0.0345	0.233	0.140	70.0
Lung ($\times 10^3$)	0.410	2.72	1.64	772.0
		Percentage of body weight		
Liver	4.0	4.0	4.0	3.14
Rapidly perfused	5.0	5.0	5.0	3.71
Slowly perfused	78.0	75.0	75.0	62.1
Fat	4.0	7.0	7.0	23.1
Flows (liters/hr)				
Alveolar ventilation	2.32	5.10	3.50	348.0
Cardiac output	2.32	5.10	3.50	348.0
		Percentage of cardiac output		
Liver	0.24	0.24	0.20	0.24
Rapidly perfused	0.52	0.52	0.56	0.52
Slowly perfused	0.19	0.19	0.19	0.19
Fat	0.05	0.05	0.05	0.05
Partition coefficients				
Blood/air	8.29	19.4	22.5	9.7
Liver/blood	1.71	0.732	0.840	1.46
Lung/blood	1.71	0.732	0.840	1.46
Rapidly perfused/blood	1.71	0.732	0.840	1.46
Slowly perfused/blood	0.960	0.408	1.196	0.82
Fat/blood	14.5	6.19	6.00	12.4
Metabolic constants				
V_{max} (mg/hr)	1.054	1.50	2.047	118.9
K_m (mg/liter)	0.396	0.771	0.649	0.580
KF (hr^{-1})	4.017	2.21	1.513	0.53
A1	0.416	0.136	0.0638	0.00143
A2	0.137	0.0558	0.0774	0.0473

[a] Parameters correspond to the average body weight of B6C3F1 mice in the NTP bioassay (NTP, 1985).
[b] Parameters correspond to the average body weight in gas uptake studies.

and is described by an allometric equation of the form (Adolph, 1949)

$$\text{lung weight} = 0.0115 * (\text{body weight})^{0.99}.$$

Some of the ventilation rates used in this model were estimated from gas uptake studies. In these studies, animals were placed in a small chamber with a recirculating atmosphere, chemical was injected into the chamber, and the chamber concentration decay was monitored over time. At low concentrations, with soluble well-metabolized chemicals such as DCM, the loss from the chamber appears to be dependent on only alveolar ventilation rates and chamber volume. Studies with rats and hamsters enclosed in such a chamber are consistent with a ventilation rate (QP) calculated according to the equation

$$QP = 15 \text{ liters/hr } (BW)^{0.74}.$$

The use of 0.74 as the exponent for body weight (BW) was proposed by Guyton (1947), based on studies with anesthetized animals. This equation predicts an alveolar ventilation of 348 liters/hr in a 70-kg human (total ventilation = 1.5 times alveolar ventilation or 522 liters/hr). This rate of ventilation is intermediate between the value reported by the ICRP (1975) for a resting human (300 liters/hr) and the value utilized by EPA for its risk estima-

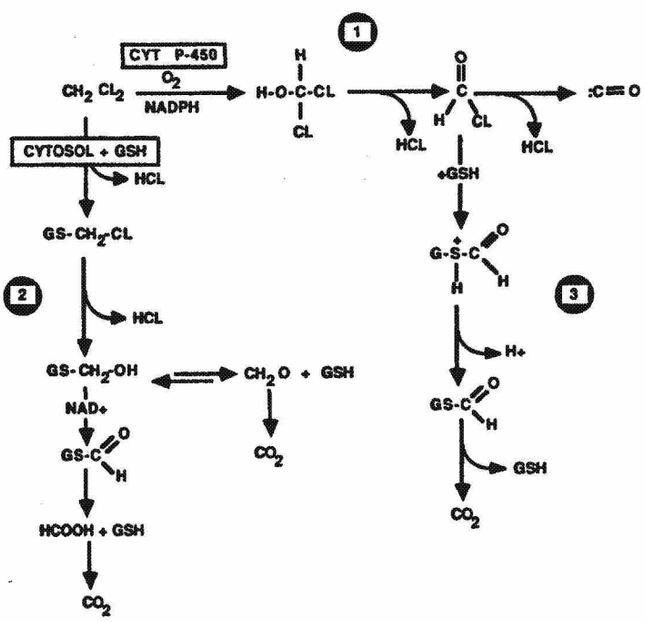

FIG. 2. Proposed metabolic pathways for methylene chloride metabolism (based on Ahmed and Anders (1978) and Kubic *et al.* (1974)). Potentially reactive intermediates are formed in each pathway: Formyl chloride in the CYT *P*-450 (MFO) pathway, and chloromethyl glutathione in the cytosolic (GST) pathway. Either metabolic pathway can produce carbon dioxide in this scheme, but only the MFO pathway yields carbon monoxide and carboxyhemoglobin.

tion (20 m^3/24 hr or 833 liters/hr) which corresponds to humans performing mild exercise.

Cardiac output (QC) was described by a similar equation:

$$QC = 15 \text{ liters/hr } (BW)^{0.74}$$

and this equation gives values consistent with those reported in the medical literature (ICRP, 1975; Davis and Mapleson, 1981).

In contrast with rats and hamsters, gas uptake studies with B6C3F1 and CD1 mice indicated that QP and QC were higher than expected from the preceding equations. In the studies with DCM, as well as recent work in our laboratory with trichloroethylene, perchloroethylene, vinyl chloride, and methylcyclohexane, we have found that chamber clearance by mice is consistent with an allometric constant of approximately 28 liters/hr. Consequently, alveolar ventilation (QP) and cardiac output (QC) in the B6C3F1 mouse were calculated according to the equations

$$QP_{mouse} = 28 \text{ liters/hr } (BW)^{0.74}$$

$$QC_{mouse} = 28 \text{ liters/hr } (BW)^{0.74}.$$

Biochemical constants (rodents). Dihalomethanes are metabolized via two pathways: (1) an oxidative pathway (Kubic *et al.*, 1974) that appears to yield CO as well as considerable amounts of CO_2 (Gargas *et al.*, 1986a; Reitz *et al.*, 1986), and (2) a glutathione-dependent pathway (Ahmed and Anders, 1978) that produces CO_2 but no CO (Fig. 2). Both pathways release 2 mol of halide ion/mol of dihalomethane consumed. The oxidative pathway (MFO) is readily saturated at concentrations of a few hundred ppm, but the glutathione *S*-transferase (GST) pathway showed no indication of saturation at inhaled concentrations up to 10,000 ppm (Gargas *et al.*, 1986a). Reactive, potentially toxic intermediates are formed in both pathways (Fig. 2).

The following procedure was employed to estimate the kinetic constants for these pathways in rodents. First the pharmacokinetic model (Fig. 1) was adapted to describe the disposition of DCM in a closed recirculating chamber. This model included both first-order (GST) and saturable pathways (MFO), as well as all the physiological constants and partition coefficients described above. Metabolism by each pathway was apportioned between lung

TABLE 2

SPECIFIC ACTIVITIES OF GLUTATHIONE *S*-TRANSFERASE AND MIXED-FUNCTION OXIDASE (MONOOXYGENASE) IN SUBCELLULAR PREPARATIONS OF RODENT AND HUMAN ORGANS, FROM LORENZ *et al.* (1984)

Species	Organ	Mixed-function oxidase	Glutathione *S*-transferase
Human			
	Liver	0.418 ± 0.157	1650 ± 480
	Lung	0.0006 ± 0.0003	78 ± 47
Sprague–Dawley rat			
	Liver	0.814 ± 0.118	1380 ± 110
	Lung	0.111 ± 0.035	77 ± 5
Syrian Golden Hamster			
	Liver	2.570 ± 0.580	4200 ± 110
	Lung	0.164 ± 0.042	325 ± 25
NMRI mouse			
	Liver	1.760 ± 0.115	5290 ± 430
	Lung	0.732 ± 0.115	727 ± 64

Note. Specific activities are given in nmol product/min/mg protein.

and liver by reference to literature data (Table 2) from Lorenz *et al.* (1984) who reported specific activities of MFO and GST in mouse, rat, hamster, and human tissues using model substrates for each enzyme (7-ethoxycoumarin for MFO and 2,5-dinitrochlorobenzene for GST).

The mass balance differential equations for the liver compartment (Appendix A) contained terms for saturable oxidative metabolism (MFO) and first-order metabolism via glutathione conjugation (GST). The corresponding equations for the lung compartment contained terms A1 and A2 which represented the relative specific activities of the enzymes (Table 2) in the two tissues such that

$$A1 = MFO_{(lung)}/MFO_{(liver)}$$

$$A2 = GST_{(lung)}/GST_{(liver)}.$$

The derivation of these equations is outlined in Appendix B.

Closed-chamber exposures of mice, rats, and hamsters were conducted with a variety of initial exposure concentrations. A description of this apparatus has been reported elsewhere (Gargas *et al.*, 1986a) and a more complete description is in press (Gargas *et al.*, 1986b). Each experiment with B6C3F1 mice employed 14 male animals, and initial concentrations were 490, 960, 2000, 3200, and 10,000 ppm DCM. Five male hamsters were employed in each experiment, with initial concentrations of 450, 1000, 1900, and 4900 ppm. Three F344 male rats were used in each exposure, with initial concentrations of 100, 500, 1000, and 3000 ppm. The concentration of DCM in the closed chamber was measured every 10 min for several hours. Optimum values of V_{max} (maximum velocity of metabolism by MFO in liver), K_m (Michaelis constant for DCM metabolism by MFO), and KF (first-order rate constant for metabolism of DCM by GST in liver) were found by minimizing the relative least squares of deviations between the actual data and the model predictions. Optimizations were performed with SIMUSOLV,[1] a computer program which combines numerical integration, optimization, and graphical display routines.[2]

These experiments give data which are rich in information about the kinetic constants. Curves from different initial concentrations are differentially affected by the values chosen for these constants. High concentration uptake is affected predominately by the value chosen for KF. Mid-range curves primarily reflect the influence of V_{max}, and low concentration curves are most sensitive to the value chosen for K_m.

Biochemical constants (humans). Values of K_m and V_{max} needed to describe the MFO pathway in humans were estimated from studies conducted at Dow Chemical Co. in which levels of DCM and carboxyhemoglobin (HbCO) in blood and of CO and DCM in expired air were measured during and following 6-hr exposures to 100 and 350 ppm DCM (Nolan and McKenna, unpublished data). These authors estimated that V_{max} in humans for the MFO pathway was 119 mg/hr and K_m was 0.58 mg/liter.

[1] SIMUSOLV is a trademark of the Dow Chemical Co.

[2] These software packages are available commercially from Mitchell and Gauthier Associates, Inc., 73 Junction Square Dr., Concord, MA 01742.

TABLE 3

ALLOMETRIC ESTIMATION OF THE KINETIC CONSTANTS FOR THE GST PATHWAY IN HUMANS

Species	KF[a] (hr^{-1})	VL[b] (ml)	KF•VL[c] (ml/hr)	BW (kg)	CLC[d] (mg/hr)
Mouse[e]	4.32	1.08	4.67	0.027	58.5
Hamster[e]	1.51	5.60	8.46	0.140	33.5
Rat[e]	2.21	9.32	20.6	0.233	57.1
Human	0.53[f]	2210	1174	70.0	60.0

[a] KF is the first-order rate constant obtained from the closed-chamber *in vivo* optimizations.

[b] VL is the estimated volume of the liver (in ml) for each of the experimental species.

[c] KF•VL is the product of columns 1 and 2.

[d] The intrinsic clearance (CLC, the clearance which would be expected in a 1-kg animal of each species if clearance were related to the 0.7 power of body weight) is calculated by dividing the clearance (KF•VL) by the body weight (BW) raised to the 0.7 power.

[e] All parameters are for the animals used in closed-chamber experiments. Mouse parameters differ from the parameters for Table 4 which were calculated for larger animals in the NTP bioassay.

[f] KF for humans was estimated by setting human CLC equal to 60.0 (approximating the highest CLC observed experimentally) and using this value to calculate KF as equal to 60 times $(70)^{0.7}$ divided by VL.

Gargas *et al.* (1986a) developed a PB-PK model for describing carboxyhemoglobin associated with metabolism of dihalomethanes to CO. This model was used in conjunction with the data of Peterson (1978) to estimate the V_{max} for the MFO pathway in humans as 137 mg/hr.

These values of V_{max} agree closely with each other and with the values obtained by allometric scaling from the rat (81.4 mg/hr) and hamster (158.6 mg/hr). The K_m for humans is also similar to the K_m obtained in the rodent species by optimizations (Table 1).

There are no data which allow direct calculation of the kinetic constant for the nonsaturable GST pathway in humans (this would require conducting exposures of several thousand ppm in humans). However, we noted that clearance (ml/hr) for the GST pathway in liver (calculated as KF•VL) appeared to possess an allometric relationship in the three rodent species. This is demonstrated by the observation that the intrinsic clearance (KF•VL divided by $(BW)^{0.7}$) is quite consistent in the three species: B6C3F1 mouse, 58.5 ml/hr/kg; hamster, 33.5 ml/hr/kg; F344 rat, 57.1 ml/hr/kg. Intrinsic clearance for humans was set equal to the highest value observed experimentally (60 ml/hr/kg), and this was used to estimate the clearance in 70-kg humans as 1174 ml/hr, corresponding to a KF of 0.53 hr^{-1} (Table 3).

Dose surrogates. The PB-PK model contains a variety of information in terms of blood and tissue concentrations of DCM, exhaled DCM, and instantaneous rates of metabolism by each pathway. The parameters which were chosen as possible dose surrogates for the toxicity of DCM were (1) integrated tissue dose as area under the tissue concentration/time curve (AUCL for liver and AUCLU for lung), (2) a virtual concentration of reactive metabolite from the MFO pathway in liver and lung tissue, and (3) a virtual concentration of reactive metabolite from the GST pathway in liver and lung tissue. These last two measures of tissue exposure were calculated by dividing the average amount of metabolite formed per day by the volume of the organ in which it was formed. Use of this type of dose surrogate has been discussed elsewhere (Andersen, 1986). The appropriate equations are

$$\text{RISK1}_{(\text{tissue})} = \text{AM1}_{(\text{tissue})}/V_{(\text{tissue})}$$

$$\text{RISK2}_{(\text{tissue})} = \text{AM2}_{(\text{tissue})}/V_{(\text{tissue})}.$$

The rationale for use of these particular surrogates is provided in Appendix C. These values are expected to be directly related to the area under the concentration time curve for the reactive intermediate in the target tissues.

RESULTS

Determination of the biochemical constants for B6C3F1 mice, CD-1 mice, F344 rats, and Syrian Golden Hamsters. Closed (recirculating)-chamber exposures of rats, hamsters, and B6C3F1 mice were conducted with a variety of initial-exposure concentrations. Model predictions and experimental

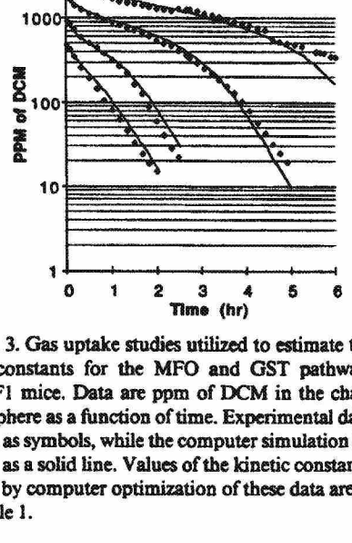

FIG. 3. Gas uptake studies utilized to estimate the kinetic constants for the MFO and GST pathways in B6C3F1 mice. Data are ppm of DCM in the chamber atmosphere as a function of time. Experimental data are shown as symbols, while the computer simulation is presented as a solid line. Values of the kinetic constants obtained by computer optimization of these data are listed in Table 1.

data are plotted for B6C3F1 mice (Fig. 3). Similar results were obtained in experiments conducted with Syrian Golden Hamsters and F344 rats (data not shown). Excellent fits were obtained for each species. The values chosen by the computer for the kinetic parameters in each species are listed in Table 1.

Validation of the model with experimental data. To test the reliability of the model, we have compared its predictions with several sets of blood concentration/time-course data. One of the strengths of physiological modeling is the ability to use the same model to predict the disposition of materials given by different routes of administration. Consequently, we have used data derived from intravenous studies as well as inhalation exposures.

The first data set (Fig. 4a) was from Angelo *et al.* (1984), who administered DCM to B6C3F1 mice intravenously at 10 and 50 mg/kg and measured the concentration in blood for periods up to 90 min postdosing. Input of DCM was simulated as a rapid infusion directly into the mixed venous blood.

In a similar fashion, the model was used to predict the blood levels of DCM in F344 rats given an intravenous dose of 10 mg/kg DCM (Fig. 4b). Blood concentrations were measured from 5 to 60 min postdosing (Andersen *et al.*, 1984).

In addition, blood levels of DCM in F344 rats inhaling 200 or 1000 ppm DCM for 4 hr were modeled (Andersen *et al.*, 1984). Blood levels of DCM were well described by the model both during the 4-hr exposure and for periods up to 120 min following cessation of exposure (Fig. 4c).

Experiments conducted with human volunteers at Dow Chemical Co. were also evaluated. In these studies, healthy volunteers were exposed to either 100 or 350 ppm of DCM for 6 hr, and samples of venous blood were collected during the exposure and for periods up to 24 hr after cessation of exposure. This simulation may be regarded as the ultimate test of animal extrapolation, and the predicted values for humans were in excellent agreement with the experimental data (Fig. 4d).

The model also predicted the appearance and elimination of DCM metabolites (Reitz *et al.*, 1986; Andersen *et al.*, 1984; Gargas *et al.*, 1986a).

Comparison of two studies of the chronic toxicity of DCM. The PB-PK model can now be used to compare the values of the relevant measures of target tissue dose during two chronic bioassays of DCM toxicity in the B6C3F1 mouse. The inhalation bioassay revealed significant increases in lung and liver tumors (NTP, 1985) while the drinking water study failed to show a dose-related increase in the incidence of either type of tumor in this same strain of mouse (Serota *et al.*, 1984a).

Six different dose surrogates were calculated for B6C3F1 mice under the conditions of exposure in these studies: (1) area under the liver concentration/time curve (AUCL), (2) area under the lung concentration/time curve (AUCLU), (3) virtual concentration of metabolites derived from the MFO pathway

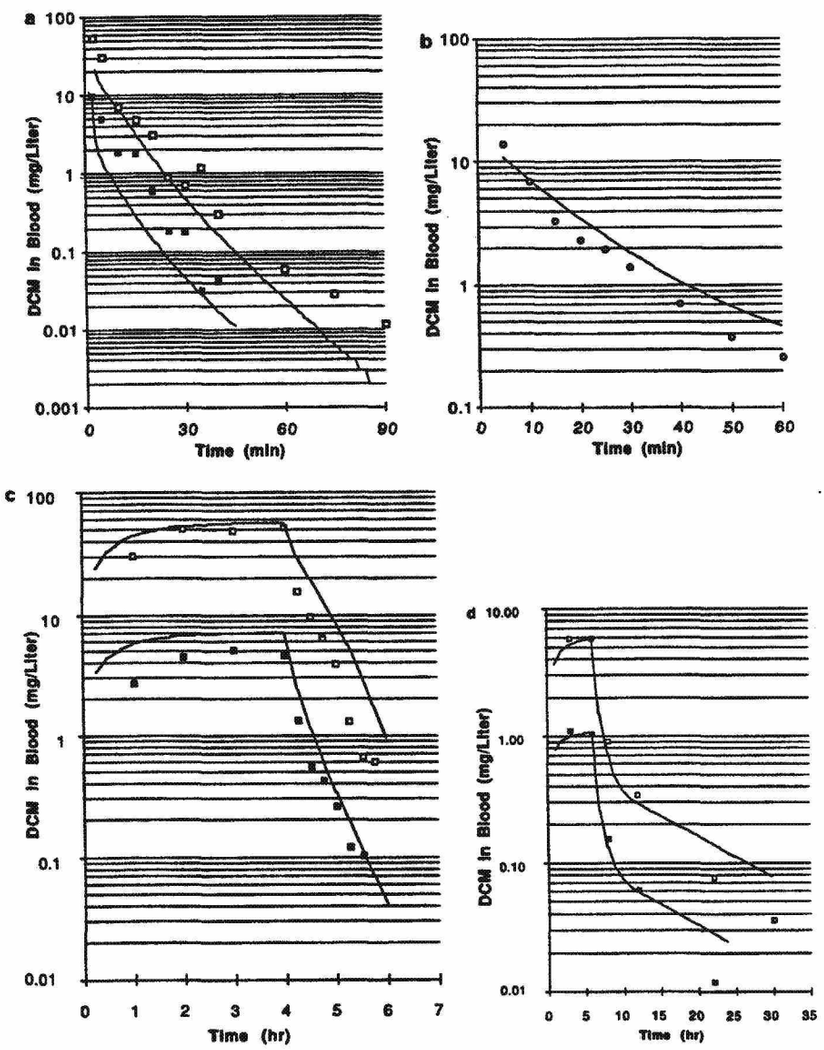

FIG. 4. Validation of the PB-PK model with experimental data. Figure 4a shows blood concentration/time data obtained in B6C3F1 mice following intravenous administration (Angelo *et al.*, 1984); Fig. 4b presents intravenous data obtained in F344 rats; Fig. 4c presents data obtained in F344 rats during and following inhalation exposure; and Fig. 4d presents data obtained in humans during and following inhalation exposure. In each case, the simulated data is presented as a solid line, while the experimental data is shown with closed or open symbols.

in liver (RISK1L), (4) virtual concentration of metabolites derived from the MFO pathway in lung (RISK1LU), (5) virtual concentration of metabolites derived from the GST pathway in liver (RISK2L), and (6) virtual concentration of metabolites derived from the GST pathway in lung (RISK2LU).

Dose surrogates related to the MFO path-

TABLE 4

COMPARISON OF AVERAGE DAILY VALUES OF DOSE SURROGATES AND TUMOR INCIDENCES IN LUNG AND LIVER TISSUES OF FEMALE B6C3F1 MICE IN TWO CHRONIC BIOASSAYS OF METHYLENE CHLORIDE (DCM)

	Control	Inhalation (4000 ppm)	Inhalation (2000 ppm)	Drinking water (250 mg/kg/day)
Liver				
RISK1L[a,g]	0.0	3701.0	3575.0	5197.0
RISK2L[b,g]	0.0	1811.0	851.0	15.1
AUCL[c,h]	0.0	771.0	362.0	6.4
Tumors (%)	6.0[i]	83.0[i]	33.0[i]	6.0[i]
Lung				
RISK1LU[d,g]	0.0	1583.0	1531.0	1227.0
RISK2LU[e,g]	0.0	256.0	123.0	1.0
AUCLU[f,h]	0.0	794.0	381.0	3.1
Tumors (%)	6.0[i,j]	85.0[i,j]	63.0[i,j]	8.0[i,j]

[a] RISK1L is the dose surrogate related to MFO activity in the liver.
[b] RISK2L is the dose surrogate related to GST activity in the liver.
[c] AUCL is the dose surrogate related to concentration of DCM in the liver.
[d] RISK1LU is the dose surrogate related to MFO activity in the lung.
[e] RISK2LU is the dose surrogate related to GST activity in the lung.
[f] AUCLU is the dose surrogate related to concentration of DCM in the lung.
[g] Units are mg of DCM metabolized/liter tissue.
[h] Units are (mg/liter)•hr.
[i] Tumor incidence (combined benign and malignant) reported as % of animals examined.
[j] Combined incidence of alveolar/bronchiolar adenomas and carcinomas.

way were nearly identical in the two studies. Values of RISK1L (the liver dose surrogate) in units of mg/liter/24 hr are 3575 and 3701 after exposure to 2000 and 4000 ppm, respectively, while the value of RISK1L is 5197 in mice consuming DCM in drinking water at the rate of 250 mg/kg/day. Similarly, the values of RISK1LU (the lung dose surrogate) are 1531 and 1583 after 2000 and 4000 ppm, respectively, while RISK1LU is 1227 in mice consuming DCM in drinking water at the rate of 250 mg/kg/day (Table 4).

By contrast, dose surrogates related to the activity of the GST pathway showed significant differences in the two studies. Values of RISK2L (the liver dose surrogate) are 851 and 1811 after exposure to 2000 and 4000 ppm, respectively, while the value of RISK2L is only 15.1 in mice consuming DCM in drinking water at the rate of 250 mg/kg/day. Similarly, the values of RISK2LU (the lung dose surrogate) are 123 and 256 after 2000 and 4000 ppm, respectively, while RISK2LU is only 1.00 in mice consuming DCM in drinking water at the rate of 250 mg/kg/day (Table 4).

Dose surrogates related to concentrations of DCM itself in the target tissues also showed significant differences in the two studies. Values of AUCL (area under the liver concentration curve) were 362 and 771 after 2000 and 4000 ppm, respectively, and values of AUCLU (area under the lung curve) were 381 and 794, respectively, after these same exposures. By contrast, levels of these parameters were 6.4 and 3.1, respectively, in the 250 mg/kg/day drinking water study (Table 4).

The PB-PK analysis indicates that the tumor incidences observed in the two studies are inconsistent with the hypothesis that reactive intermediates from the MFO pathway are involved in the tumorigenicity of DCM,

but are consistent with two other hypotheses: (1) that tumorigenicity is related to the production of reactive intermediates by the GST pathway and (2) that tumorigenicity is related to the presence of DCM in the target organs.

Relationship of dose surrogate values to administered dose. The PB-PK model may now be utilized to calculate the values of the toxicologically relevant chemical species in various tissues under a variety of exposure conditions. For example, the value of the liver dose surrogate related to the GST pathway (RISK2L) in B6C3F1 mice and in humans following inhalation of various concentrations of DCM for 6 hr/day is plotted in Fig. 5a.

The calculated dose surrogates are displayed on a log/log plot for exposure concentrations from 1 to 4000 ppm. Dose surrogate values for B6C3F1 mice are represented by the heavy solid line, while dose surrogate values for humans are represented by the heavy dashed line. Dose surrogate values which would be obtained by linear extrapolation of data from the 4000-ppm mouse exposure are depicted as a lighter solid line in this and other figures. Dose surrogate values calculated from the PB-PK model are close to those estimated by linear extrapolation with the mouse above 1000 ppm, but deviate from linearity in the region below 1000 ppm. The nonlinearity in the curve is apparent in the region where the MFO pathway saturates. Saturation of MFO makes a larger percentage of the DCM available for metabolism by the GST pathway, resulting in a disproportionate increase in RISK2L at exposure concentrations above 100 ppm. The curve for liver dose surrogate values in humans (exposed 6 hr/day) also displays a nonlinearity in the region between 100 and 1000 ppm, although this is less pronounced than in mice. The values of human dose surrogates are lower than mouse dose surrogates throughout the entire exposure range.

Figure 5b presents the values of the lung dose surrogate related to GST (RISK2LU) in mice and in humans exposed to various concentrations of DCM in air. In this case, the nonlinearity in the mouse dose surrogate curve is of smaller magnitude than that in mouse liver, indicating a smaller effect of MFO on the material available for GST. As with RISK2L, the value of human RISK2LU is lower than that of mouse RISK2LU at all concentrations because of the lower activity of GST in human lung relative to that in mouse lung (Table 2).

For drinking water exposures, RISK2L and RISK2LU are plotted vs concentration of DCM present in water in milligrams/liter (Figs. 5c,d). Water consumption for the two species was estimated according to the equation

$$\text{water consumption} = 0.102 * (\text{BW})^{0.7}$$

which results in an estimated water consumption of 2.0 liters/day for 70-kg humans and 9.7 ml/day for 34.5-g mice.

A nonlinearity in each of those dose surrogate curves (RISK2L and RISK2LU; mice and humans) is evident at concentrations above 1000 mg/liter. Dose surrogate values for the mouse drinking water simulations with 10,000 mg/liter are lower than values of the same parameter for mice inhaling 4000 ppm DCM per day (Figs. 5c, 5a; 5d, 5b). In each case, the dose surrogates for humans are lower than the dose surrogates for mice when the two species consume water with the same concentration of DCM.

Dose surrogate values for parameters related to the MFO pathway in liver (RISK1L) when DCM is present in inhaled air are displayed in Fig. 6a. Nonlinearities are apparent in the region of 100–1000 ppm. MFO products do not increase appreciably in mice above 200–400 ppm. MFO products increase, but to a less than proportionate degree, as DCM levels rise above 1000 ppm in humans due to fat storage with postexposure metabolism (Clewell and Andersen, 1985).

Dose surrogate values for parameters related to area under the liver concentration/

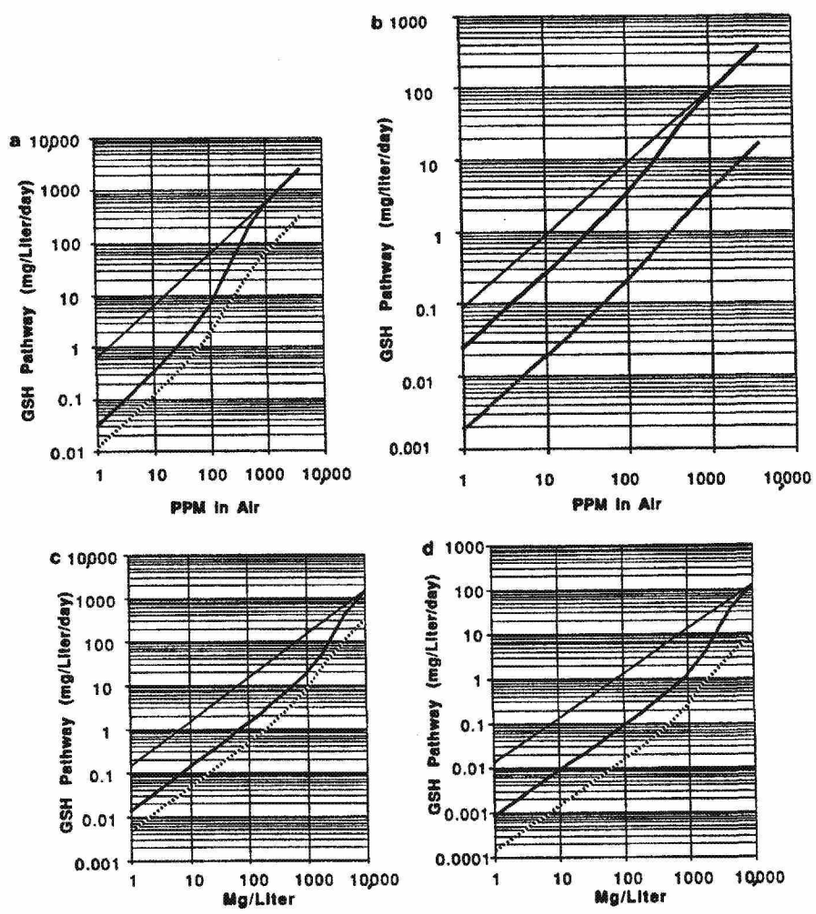

FIG. 5. Predicted relationship of the dose surrogates associated with the GST pathway to external dose. Figs. 5a and 5b show the values of the dose surrogates in B6C3F1 mice and humans during inhalation exposure (6 hr/day) in the liver and lung, respectively. Figures 5c and 5d show these same dose surrogates in B6C3F1 mice and humans consuming water with DCM dissolved at various levels. Dose surrogates for mice are shown as a heavy solid line, while dose surrogates for humans are shown as a heavy dashed line. In each case, a reference line depicting a linear extrapolation from the highest administered dose of DCM is shown as a light, solid line for comparison. Units for the *Y*-axis are mg metabolized per liter tissue per 24 hr.

time curve (AUCL) in animals inhaling DCM are displayed in Fig. 6b. Nonlinearities are evident in the region of 100–1000 ppm. The values of this particular dose surrogate are higher for humans than for mice, but in each case there is a marked difference between the dose surrogate values obtained by linear extrapolation from 4000 to 1 ppm and the values calculated by the PB-PK model for 1 ppm (Fig. 6b).

DISCUSSION

A great number of uncertainties are involved in the formulation of human risk esti-

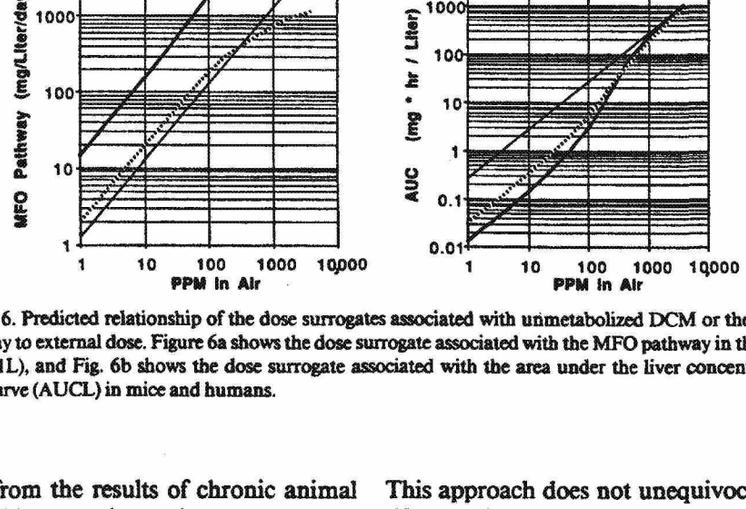

FIG. 6. Predicted relationship of the dose surrogates associated with unmetabolized DCM or the MFO pathway to external dose. Figure 6a shows the dose surrogate associated with the MFO pathway in the liver (RISK1L), and Fig. 6b shows the dose surrogate associated with the area under the liver concentration time curve (AUCL) in mice and humans.

mations from the results of chronic animal studies. This paper is not intended to be a comprehensive enumeration and discussion of all these factors. It is restricted to a discussion of the role that PB-PK models can play in relating the "external dose" of DCM to tissue doses in the target organs of various species under specific exposure scenarios.

Advantages of PB-PK. Development of a PB-PK analysis offers significant advantages over conventional pharmacokinetic analysis. In conventional pharmacokinetics, time-course curves are obtained for concentration of a parent chemical or metabolite(s) in blood or in some other body compartment. The resulting curves are then described by mathematical curve-fitting techniques, resulting in models which are more dependent on the mathematics employed than on the animal system being studied. Such descriptions are best suited to interpolation or limited extrapolation. By contrast, PB-PK models are designed to predict kinetic behavior over a broad range of doses and exposure regimens (Clewell and Andersen, 1985).

Differentiation of metabolic pathways. In this study gas uptake methods have been utilized to determine the kinetic constants for two pathways of dihalomethane metabolism. This approach does not unequivocally identify a particular metabolic pathway with a kinetic process. Other chemical studies are necessary to make this identification.

Such studies were reported previously by Gargas *et al.* (1986a), who evaluated the metabolism of five dihalomethanes. In that work, carboxyhemoglobin production (a unique product of the MFO pathway) and bromide ion liberation were correlated with the gas uptake studies. The high-affinity saturable pathway was shown to be the oxidative reaction (MFO) which produces, among other metabolites, carbon monoxide. The first-order pathway was shown to be dependent on glutathione concentration. These studies link the two uptake processes observed *in vivo* in the gas uptake studies with the MFO and GST pathways.

Model validation. The goal of these experiments was to determine whether the model could successfully predict a broad range of kinetic behavior. It must be emphasized that the validation was not an exercise in curve-fitting; model parameters were not "fiddled" in an attempt to hit all the data points. Nevertheless, the degree of agreement between the model predictions and the blood concentration time-course data, obtained from three

laboratories and through two routes of administration, is remarkable (Figs. 4a–d). In particular, it is noteworthy that the disposition of DCM in humans is described accurately by the model.

Basic assumptions. Implicit in every risk assessment procedure are some fundamental assumptions about the manner in which chemical treatments affect the carcinogenic process. In the discussion which follows it is assumed that treatments which produce equivalent average daily tissue exposures of the relevant chemical species (dose surrogates) in target organs will produce equivalent effects on the carcinogenic process in each species. Factors such as longevity of the various species and latent periods for tumor induction, which may also be biologically important, are not considered. In the PB-PK analysis, no attempt is made to incorporate a factor converting external dose to milligrams/surface area when extrapolating among species. The PB-PK model already incorporates appropriate factors for interspecies scaling. Furthermore, empirical generalizations such as converting doses to milligrams/meter^2 fail to consider the role of metabolic processes in increasing or decreasing toxicity, and may lead to serious errors in interspecies extrapolation.

Hypothesis generation. Although the PB-PK model is capable of quantitatively describing the levels of DCM and its metabolites in the body, it is not capable of determining by itself which of these parameters is likely to be related to the tumorigenicity of DCM. To make this judgment, it is necessary to incorporate pertinent biological and chemical information from other nonpharmacokinetic experiments. At the outset, we considered three possible hypotheses for the mechanism of action of DCM:

(1) Tumorigenicity of DCM is related to the presence of DCM in target tissues (i.e., area under the tissue concentration/time curves).

(2) Tumorigenicity of DCM is related to the production of metabolites of DCM derived from the MFO pathway in target tissues.

(3) Tumorigenicity of DCM is related to the production of metabolites of DCM derived from the GST pathway in target tissues.

The first hypothesis was rejected on mechanistic considerations. The chemical reactivity of DCM is low, and there is no evidence that parent material is capable of the types of biological interactions with macromolecules which Miller and Miller (1966) have found to be prevalent in the action of chemical carcinogens. However, both of the metabolic pathways produce potentially reactive intermediates which might be involved in the tumorigenic process (Fig. 2).

There are several reasons for believing that metabolism by MFO is not involved in the tumorigenicity of DCM. First, it is clear that the incidence of most of the treatment-related tumors increases as the exposure concentration is raised from 2000 to 4000 ppm (Table 4). However, it has been demonstrated that HbCO, a major product of MFO activity, does not increase in rats or hamsters as exposure levels of DCM are raised above 500 ppm (McKenna *et al.*, 1982; Burek *et al.*, 1984).

In addition, Green (1983) has separated enzymes from the MFO and GST pathways and studied their ability to metabolically activate DCM *in vitro.* He found that cytosolic preparations from rat liver (containing GST) significantly increased the yield of bacterial mutations in *Salmonella typhimurium* exposed to DCM. However, rat liver microsomes rich in MFO failed to show this effect. Rannug *et al.* (1978) have observed that GST increases the mutagenicity of a similar compound, 1,2-dichloroethane, in *in vitro* studies.

Hypothesis testing. Finally, as already discussed under Results, the PB-PK model may be utilized to compare the levels of dose sur-

rogates from each pathway in the chronic studies of DCM administered by inhalation (NTP, 1985) or by drinking water (Serota *et al.*, 1984a). Significant increases in the incidence of lung and liver tumors were observed in the inhalation study, but no significant increases in these tumors were seen in the drinking water study. This correlates well with the yield of the GST metabolites in the two studies (levels of GST dose surrogates were much higher in the inhalation vs the drinking water study), but is inconsistent with the activity of the MFO pathway (levels of MFO dose surrogates were equivalent in the two studies; Table 4).

These results should not be taken as indicating that the primary mechanism by which DCM increases tumorigenicity in the mouse is necessarily through direct interaction of GST metabolites with genetic material (i.e., a genotoxic effect). Genotoxicity of DCM to mammalian cells has been very low in a number of carefully conducted experiments (Schumann, 1984; Sivak, 1984). However, it does appear that the GST pathway is somehow related to the increased tumor incidences observed in B6C3F1 mice exposed to DCM.

Allometric scaling of the constants for the GST pathway. Most of the parameters utilized in the model have come directly from the medical literature or from experiments conducted in our laboratories. However, because *in vivo* determinations of the activity of the GST pathway in humans would involve exposing humans to high concentrations of DCM, the *in vivo* activity of the GST pathway in humans was estimated by allometric scaling of the rodent data.

Use of allometric scaling is supported by the observation that allometric scaling of the GST pathway worked reasonably well in the three rodent species (intrinsic clearances (CLC) by this pathway were nearly identical for mouse, hamster, and rat; Table 3, last column), as well as the observation that allometric scaling was reasonably successful for the MFO pathway in all four species (see estimation of biochemical constants (humans) under Methods).

Further refinement of the PB-PK model will be made when *in vitro* constants for the metabolism of DCM by MFO and GST enzymes in liver and lung tissues of mice, rats, hamsters, and humans are obtained. Such studies are currently under way in other laboratories (Trevor Green, personal communication, 1986).

PB-PK risk analysis. The difference between a PB-PK-based risk assessment and a conventional risk assessment is that "internal dose" is calculated by the model rather than assumed to be linearly related to external dose and body surface area.

Use of a PB-PK analysis in risk assessment is not dependent on use of any particular model to relate internal dose and tumorigenicity (e.g., One Hit, Probit, Weibull). PB-PK models may be employed with any of the currently available models. Use of PB-PK in risk assessment does not imply an acceptance or rejection of any specific hypothesis of carcinogenicity; it simply provides a more accurate method for estimating the "internal dose."

Comparison with conventional risk analysis. The differences between risk assessments based on PB-PK and risk assessments based on procedures such as those recommended by Singh *et al.* of the EPA (1985) in their addendum to the "Health Assessment Document for Dichloromethane" may be directly calculated. In the model used by the EPA, risk is a linear function of dose, and so the ratio of the extrapolated doses would approximate the ratio of the estimated risks. If nonlinear dose–response models were used, the relationship of risks would be more complex.

Two specific situations are discussed: (1) extrapolating from data obtained in mice inhaling 4000 ppm, 6 hr/day, to predict the internal dose in humans inhaling 1 ppm for the same period, and (2) extrapolating from data obtained in mice inhaling 4000 ppm, 6 hr/

day, to predict the internal dose in humans consuming 2 liters/day of water containing 1 mg/liter DCM.

Dose surrogates related to the activity of GST (RISK2L) in the liver of humans and mice during inhalaion exposure are displayed in Fig. 5a. Inspection of this curve reveals that dose surrogates in the mouse at 1 ppm are 20.8-fold lower than a linear extrapolation would predict. Furthermore, the PB-PK model reveals that human dose surrogates are 2.74-fold lower than mice for a 1-ppm exposure.

By contrast, the EPA has suggested (EPA, 1983, pp. 5-98 to 5-99) that values extrapolated linearly from 4000 ppm in the mouse should be increased by 2.95-fold to reflect differences in the breathing rates and relative surface areas of the two species. The result is that the internal dose calculated by the PB-PK model is approximately 170-fold (20.8 × 2.74 × 2.95) lower than the internal dose estimated by the EPA procedure (Table 5).

Similarly, the dose surrogates related to activity of the GST pathway in lung tissue (RISK2LU) are depicted in Fig. 5b. In this case, the PB-PK model calculates internal concentrations at 1 ppm which are 3.71-fold lower than a linear extrapolation of mouse data from 4000 ppm. Human dose surrogates at 1 ppm are 13.1-fold lower than the mouse at 1 ppm (because of the relatively low levels of GST in human lung tissue). The result in this case is that the internal dose calculated by the PB-PK model for humans exposed to 1 ppm DCM is approximately 140-fold lower than the internal dose estimated by the EPA (Table 5).

In the case of drinking water exposures, the PB-PK model calculates an internal dose which is approximately 210-fold lower for lung dose surrogates and 45-fold lower for liver dose surrogates than with the "linear/surface area" procedure (Table 5).

It appears likely that the document prepared by Singh *et al.* of the EPA (which is representative of the approaches employed by other federal agencies as well) significantly overestimates the risk in humans exposed to low concentrations of DCM. This overestimation comes from two sources: (1) failure to consider the effect of enzyme saturation at high levels such as those employed in the NTP bioassay, and (2) failure to recognize that because of their relatively lower levels of metabolic enzymes, humans may be expected to be less sensitive to DCM than the rodent species.

Relating cancer risk to internal dose involves the assumption that all species will be equally sensitive to a given target tissue dose.

TABLE 5

AVERAGE DAILY VALUES FOR INTERNAL CONCENTRATION (DOSE SURROGATES) CALCULATED BY THE PB-PK MODEL AND THE "LINEAR/SURFACE" AREA EXTRAPOLATION PROCEDURES

	Linear surface area	PB-PK model	Ratio
Mouse (4000 ppm, inhalation)			
Liver	1811.0[a,b]	1811.0[a,b]	—
Lung	255.0[a,b]	255.0[a,b]	—
Human (1 ppm, inhalation)			
Liver	1.34	0.00804[b]	167
Lung	0.188	0.00131[b]	144
Human (1 mg/liter, drinking water)			
Liver	0.211	0.00468	45.1
Lung	0.0298	0.00014	213

[a] The PB-PK model output for 4000 ppm was used as the basis for the extrapolation procedure. In each case, extrapolation is from the data obtained with the B6C3F1 mouse exposed to 4000 ppm methylene chloride (DCM) for 6 hr/day, 5 days/week, throughout its lifetime. Two specific types of extrapolation are performed: (1) for humans inhaling 1 ppm DCM for the same period, and (2) for humans drinking water containing 1 mg/liter of DCM.

[b] Dose surrogate values in this table differ from those shown in Fig. 5 due to a factor of 5/7 applied to adjust 5 days/week exposure instead of 7 days/week exposure.

In fact, this assumption may not be reasonable when the B6C3F1 hybrid mouse is compared with other species and/or strains. For example, hamsters were subjected to a bioassay very similar to that conducted by the NTP for B6C3F1. However, even though PB-PK analysis estimated that target tissue doses in the hamster were nearly equivalent to those achieved in the B6C3F1 mouse (data not shown), excess tumors (at any site) were not observed in the hamster bioassay (Burek *et al.*, 1984). It appears that production of a particular target tissue dose may be "necessary but not sufficient" to cause a tumorigenic response. Many additional factors must be considered when formulating risk estimations, and Park and Snee (1983) have proposed a technique for combining quantitative and qualitative factors.

In summary, a unified, physiologically based pharmacokinetic model for DCM which encompasses data from a variety of sources has been developed. This model may be used to strengthen the scientific basis of risk assessment for DCM, improve experimental design of chronic studies, and give insight into mechanisms of toxicity and metabolism. This approach is not uniquely applicable to DCM, but could easily be employed with other materials. Many uncertainties remain in the risk assessment process, but risk assessments which properly consider the role of physiologically based pharmacokinetics should be significantly more reliable than those which do not.

APPENDIX A

Differential equations and abbreviations for the various tissue compartments utilized in the PB-PK model which are different from those reported by Ramsey and Andersen (1984) are listed below:

Gas Exchange Compartment

$$CA1 = (QC*CV + QP*CI)/(QC + QP/PB)$$

$$CX = CA1/PB$$

$$CA = CLU/PLU$$

Lung Tissue Compartment (Where Metabolism Occurs)

$$dALU\,dt = QC*(CA1 - CA) - dAM1LU - dAM2LU$$

$$dAM1LU\,dt = A1*V_{max}*CA*(VLU/VL)/(K_m + CA)$$

$$dAM2LU\,dt = A2*KF*CA*VLU$$

$$ALU = \text{Integral}\,(dALU\,dt)$$

$$CLU = ALU/VLU$$

$$AUCLU = \text{Integral}\,(CLU\,dt)$$

Liver Compartment

$$dAL\,dt = QL*(CA - CVL) - dAM1L - dAM2L + KZER$$

$$dAM1L\,dt = (V_{max}*CVL)/(K_M + CVL)$$

$$dAM2L\,dt = KF*CVL*VL$$

$$AL = \text{Integral}\,(dAL\,dt)$$

$$CL = AL/VL$$

$$CVL = CL/PL$$

$$AUCL = \text{Integral}\,(CL\,dt)$$

Abbreviations used in the model are defined below:

Concentrations (in milligrams/liter)

- CA1 Concentration of DCM in blood leaving gas exchange compart.
- CA Concentration of DCM in arterial blood.
- CI Concentration of DCM in inhaled air.
- CL Concentration of DCM in liver tissue.
- CLU Concentration of DCM in lung tissue.
- CV Concentration of DCM in mixed venous blood.
- CVL Concentration of DCM in venous blood leaving liver.

CX Concentration of DCM in alveolar air.

Flows (in liters/hour)

QP Alveolar ventilation rate.
QC Cardiac output.
QL Flow through liver compartment.

Amounts (in milligrams of DCM)

ALU Amount of DCM in the lung compartment.
AL Amount of DCM in the liver compartment.
AM1L Amount of DCM metabolized by MFO in liver
AM2L Amount of DCM metabolized by GST in liver
AM1LU Amount of DCM metabolized by GST in lung.
AM2LU Amount of DCM metabolized by GST in lung.

Partition Coefficients

PB Blood/air partition coefficient.
PL Liver/blood partition coefficient.
PLU Lung/blood partition coefficient.

Volumes (in liters)

VL Volume of liver.
VLU Volume of lung.

Miscellaneous

A1 Ratio of MFO activity in lung to MFO activity in liver.
A2 Ratio of GST activity in lung to GST activity in liver.
AUCL Area under the concentration time curve in the liver.
AUCLU Area under the concentration time curve in the lung.
KF First-order rate constant for GST pathway.
K_m Michaelis constant.
KZER Zero-order rate of input of DCM to liver.
V_{max} Maximum velocity of metabolism by MFO.

APPENDIX B

Apportioning Metabolism between Lung and Liver

Metabolism occurs by two pathways in each of two tissues: liver and lung. Total metabolism, determined by the gas uptake experiments, is apportioned between these tissues (i.e., it is assumed that metabolism in other tissues is negligibly small). In the mass balance differential equations the liver is referenced to its own metabolic constants. Lung is then referenced to the liver constants using the observed ratios of enzyme specific activities (A1 and A2) for each pathway (Lorenz *et al.*, 1984).

Saturable (MFO) Pathway

The rate of production of metabolities in the liver is

$$\text{dAM1L}/dt = V_{max} * \text{CVL}/(K_m + \text{CVL})$$

$$V_{max} = \text{SA1L} * \text{VL}.$$

In lung we have

$$\text{dAM1Lu}/dt = V_{max}\text{Lu} * \text{CA}/(K_m + \text{CA})$$

$$V_{max}\text{Lu} = \text{SA1Lu} * \text{VLu}.$$

Rewriting V_{max}Lu in terms of the ratio of organ-specific activities (A1 = SA1Lu/SA1L):

$$V_{max}\text{Lu} = \text{A1} * \text{SA1L} * \text{VLu}.$$

Substituting for SA1L in this equation:

$$V_{max}\text{Lu} = (\text{A1} * V_{max} * \text{VLu})/\text{VL}.$$

Assuming that K_m (the Michaelis constant) is equal in each tissue:

$$\text{dAM1Lu}/dt = \text{A1} * (\text{VLu}/\text{VL}) * \text{V}_{max} * (\text{CA}/(K_m + \text{CA})).$$

Glutathone - Transferase - Mediated Pathway

The rate of production of metabolites by the GST pathway in liver is

$$\text{dAM2L}/dt = V_{max}2 * \text{CVL}/(K_m2 + \text{CVL}).$$

Under first-order conditions where $K_m2 \gg \text{CVL}$, this becomes

$$\text{dAM2L}/dt = V_{max}2 * \text{CVL}/K_m2 = \text{SA2L} * \text{VL} * \text{CVL}/K_m2.$$

Defining the first-order rate constant KF as $(\text{SA2L}/K_m2)$,

$$\text{dAM2L}/dt = \text{KF} * \text{VL} * \text{CVL}.$$

For the lung tissue compartment (again assuming equal K_m's in the two tissues), under first-order conditions where $K_m2 \gg \text{CA}$:

$$d\text{AM2Lu}/dt = V_{max}2\text{Lu} * \text{CA}/(K_m2 + \text{CA}) = \text{SA2Lu} * \text{VLu} * \text{CA}/(K_m2 + \text{CA}) = \text{SA2Lu} * \text{VLu} * \text{CA}/K_m2.$$

*Substituting SA2Lu = (A2 * SA2L) and KF = (SA2L/K_m2)*, we obtain

$$\text{dAM2Lu}/dt = \text{A2} * \text{KF} * \text{CA} * \text{VLu}.$$

APPENDIX C

Choice of Dose Surrogates

Use of the PB-PK model for risk assessment and extrapolations requires calculation of the integrated tissue dose of parent chemical and also of several reactive metabolities that are too short-lived to measure directly. These metabolites (B) can be considered as intermediates in a general metabolic scheme:

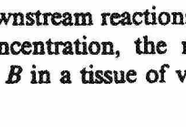

When all downstream reactions of B are linear with concentration, the mass balance equation for B in a tissue of volume V_t becomes

$$V_t * (dB/dt) = \text{Rate1} - (k_1 * B * V_t + k_2 * B * V_t + \cdots + k_i * B * V_t).$$

The concentration of a highly reactive chemical intermediate which does not accumulate will rapidly attain a steady-state condition,

$$V_t * (dB/dt) = 0$$

allowing solution of Eq. (ii) for the steady-state concentration of B, B_{ss}.

$$B_{ss} = \text{Rate1}/\sum_{i=1}^{n} (k_i * V_t).$$

If B is highly reactive and the $\Sigma\, k_i * V_t$ is large, this equation will be a good approximation of B_t during the entire exposure period. This equation can be integrated to give the expected integrated tissue exposure to the intermediate, B:

$$\int_0^t B_t dt = \int_0^t B_{ss} dt = \int_0^t \frac{\text{Rate1}\, dt}{V_t}.$$

This relationship shows that integrated tissue dose of toxic metabolite is proportional to the integral of the rate of formation of B divided by tissue volume. In this paper, integrated rate/V_t is used as a surrogate of tissue exposure to reactive intermediates. Interspecies comparisons using this dose surrogate assume that $\Sigma\, k_i * V_t$ is similar in various species.

The pathways for disappearance of B may be capacity-limited (i.e., dose dependent) at high reaction rates. Examples of this behavior occur with vinyl chloride, acetaminophen,

and ethylene dichloride where reactive metabolites eventually deplete glutathione. Estimation of tissue dose with these chemicals requires that the time dependence of GSH concentrations be known or modeled. This complication is unnecessary with DCM since GSH is regenerated when DCM is metabolized by the GST pathway (Fig. 2).

REFERENCES

ADOLPH, E. F. (1949). Quantitative relations in the physiological constitutions of mammals. *Science* **109**, 579–585.

AGIN, G. L., AND BLAU, G. E. (1982). Application of DACSL (Dow Advanced Continuous Simulation Language) to the design and applications of chemical reactor systems. *Amer. Inst. Chem. Eng. Symp. Ser. No. 214* **78**, 108–118.

AHMED, A. E., AND ANDERS, M. W. (1978). Metabolism of dihalomethanes to formaldehyde and inorganic halide. I. *In vitro* studies. *Drug. Metab. Dispos.* **4**, 357–361.

ANDERSEN, M. E., ARCHER, R. L., CLEWELL, H. J., AND MACNAUGHTON, M. G. (1984). A physiological model of the intravenous and inhalation pharmacokinetics of three dihalomethanes. *Toxicologist* **4**, 443.

ANGELO, M. J., BISCHOFF, K. B., PRITCHARD, A. B., AND PRESSER, M. A. (1984). A physiological model for the pharmacokinetics of methylene chloride in B6C3F1 mice following i.v. administration. *J. Pharmacol. Biopharmacol.* **12**, 413–436.

BUREK, J. D., NITSCHKE, K. D., BELL, T. J., WASKERLE, D. L., CHILDS, R. C., BEYER, J. D., DITTENBER, D. A., RAMPY, L. W., AND MCKENNA, M. J. (1984). Methylene chloride: A 2-year inhalation toxicity and oncogenicity study in rats and hamsters. *Fundam. Appl. Toxicol.* **4**, 30–47.

CASTER, W. O., PONCELET, J., SIMON, A. B., AND ARMSTRONG, W. D. (1956). Tissue weights of the rat. I. Normal values determined by dissection and chemical methods. *Proc. Soc. Exp. Biol. Med.* **91**, 122–126.

CLEWELL, H. J., AND ANDERSEN, M. E. (1985). Risk assessment extrapolations and physiological modeling. In *Advances in Health Risk Assessment for Systemic Toxicants and Chemical Mixtures.* Princeton Scientific Publishers, Princeton, NJ.

DAVIS, N. R., AND MAPLESON, W. W. (1981). Structure and quantification of a physiological model of the distribution of injected agents and inhaled anaesthetics. *Brit. J. Anaesth.* **53**, 399–404.

EPA (1983). Health Assessment Document for Dichloromethane (Methylene Chloride). EPA-600/8-82-004B.

FISEROVA-BERGEROVA, V. (1975). Mathematical modeling of inhlation exposure. *J. Combust. Toxicol.* **3**, 201–210.

FRANTZ, S. W., AND WATANABE, P. G., (1983). Tetrachloroethylene: Balance and tissue distribution in male Sprague–Dawley rats by drinking water administration. *Toxicol. Appl. Pharmacol.* **69**, 66–72.

GARGAS, M. L., CLEWELL, H. J., AND ANDERSEN, M. E. (1986a). Metabolism of inhaled dihalomethanes *in vivo:* Differentiation of kinetic constants for two independent pathways. *Toxicol. Appl. Pharmacol.* **87**, 211–223.

GARGAS, M. L., ANDERSEN, M. E., AND CLEWELL, H. J., III (1986b). A simulation analysis of gas uptake data. *Toxicol. Appl. Pharmacol.* **86**, 341–352.

GREEN, T. (1983). The metabolic activation of dichloromethane and chlorofluoromethane in a bacterial mutation assay using *Salmonella typhimurium. Mutat. Res.* **118**, 277–288.

GUYTON, A. C. (1947). Respiratory volumes of laboratory animals. *Amer. J. Physiol.* **150**, 70–77.

International Commission on Radiation Protection (ICRP) (1975). *Report of the Task Group on Reference Man,* ICRP Publ. 23, (W. S. Snyder *et al.*, Eds.). Pergamon, Elmsford, NY.

KUBIC, V. L., ANDERS, M. W., ENGEL, R. R., BARLOW, C. H., AND CAUGHEY, W. S. (1974). Metabolism of dihalomethanes to carbon monoxide. I. *In vivo* studies. *Drug Metab. Dispos.* **2**, 53–57.

LEITH, D. E. (1976). Comparative mammalian respiratory mechanics. *Physiologist* **19**, 485–510.

LORENZ, J., GLATT, H. R., FLEISCHMANN, R., FERLINZ, R., AND OESCH, F. (1984). Drug metabolism in man and its relationship to that in three rodent species: Monooxygenase, epoxide hydroylase, and glutathione *S*-transferase activities in subcellular fractions of lung and liver. *Biochem. Med.* **32**, 43–56.

MCKENNA, M. J., ZEMPEL, J. A., AND BRAUN, W. H. (1982). The pharmacokinetics of inhaled methylene chloride in rats. *Toxicol. Appl. Pharmacol.* **65**, 1–10.

MILLER, E. C., AND MILLER, J. A. (1966). Mechanisms of chemical carcinogenesis: Nature of proximate carcinogens and interactions with macromolecules. *Pharmacol. Rev.* **18**, 805.

National Research Council (1986). Dose route extrapolations: Using inhalation toxicity data to set drinking water limits. In *Drinking Water and Health* (R. D. Thomas, Ed.), Vol. 6, pp. 185–236. Natl. Acad. Press, Washington, DC.

National Toxicology Program (NTP) (1985). NTP Technical Report on the Toxicology and Carcinogenesis

Studies of Dichloromethane in F-344/N Rats and B6C3F1 Mice (Inhalation Studies). NTP-TR-306 (board draft).

PARK, C. N., AND SNEE, R. D. (1983). Quantitative risk assessment: State of the art for carcinogenesis. *Amer. Statist.* **37**, 427.

PETERSON, J. E. (1978). Modeling the uptake, metabolism, and excretion of dichloromethane by man. *Amer. Ind. Hyg. J.*, **39**, 41–47.

RAMSEY, J. R., AND ANDERSEN, M. E. (1984). A physiologically based description of the inhalation pharmacokinetics of styrene in rats and humans. *Toxicol. Appl. Pharmacol.* **73**, 159–175.

RANNUG, U., SUNDVALL, A., AND RAMEL, C. (1978). The mutagenic effect of 1,2-dichloroethane on *Salmonella typhimurium*. I. Activation through conjugation with glutathione *in vitro*. *Chem. Biol. Interact.* **20**, 1.

REITZ, R. H., SMITH, F. A., AND ANDERSEN, M. E. (1986). *In vivo* metabolism of ^{14}C-methylene chloride (MEC). *Toxicologist* **6**, 260.

SATO, A., AND NAKAJIMA, T. (1979). Partition coefficients of some aromatic hydrocarbons and ketones in water, blood, and oil. *Brit. J. Ind. Med.* **36**, 231–234.

SCHUMANN, A. M. (1984). Inhalation Kinetics. Food Solvents Workshop I: Methylene Chloride. March 8–9, Bethesda, MD.

SEROTA, D., ULLAND, B., AND CARLBORG, F. (1984a). Hazelton Chronic Oral Study in Mice. Food Solvents Workshop I: Methylene Chloride. March 8–9, Bethesda, MD.

SEROTA, D., ULLAND, B., AND CARLBORG, F. (1984b). Hazleton Chronic Oral Study in Rats. Food Solvents Workshop I: Methylene Chloride. March 8–9, Bethesda, MD.

SINGH, D. V., SPITZER, H. L., AND WHITE, P. D. (1985). Addendum to the Health Assessment Document for Dichloromethane (Methylene Chloride). Updated carcinogenicity assessment of dichloromethane. EPA/600/8-82/004F.

SIVAK, A. (1984). Gentoxicological Assessment Food Solvents Workshop I: Methylene Chloride. March 8–9, Bethesda, MD.

ELSEVIER

The Science of the Total Environment 274 (2001) 37–66

the Science of the Total Environment

www.elsevier.com/locate/scitotenv

Comparison of cancer risk estimates for vinyl chloride using animal and human data with a PBPK model

Harvey J. Clewell[a,*], P. Robinan Gentry[a], Jeffrey M. Gearhart[b], Bruce C. Allen[c], Melvin E. Andersen[c]

[a] *KS Crump Group, Inc., ICF Consulting, 602 East Georgia Avenue, Ruston, LA 71270, USA*
[b] *Procter and Gamble, Cincinnati, OH, USA*
[c] *Colorado State University, Fort Collins, CO, USA*

Received 20 June 2000; accepted 25 November 2000

Abstract

Vinyl chloride (VC) is a trans-species carcinogen, producing tumors in a variety of tissues, from both inhalation and oral exposures, across a number of species. In particular, exposure to VC has been associated with a rare tumor, liver angiosarcoma, in a large number of studies in mice, rats, and humans. The mode of action for the carcinogenicity of VC appears to be a relatively straightforward example of DNA adduct formation by a reactive metabolite, leading to mutation, mistranscription, and neoplasia. The objective of the present analysis was to investigate the comparative potency of a classic genotoxic carcinogen across species, by performing a quantitative comparison of the carcinogenic potency of VC using data from inhalation and oral rodent bioassays as well as from human epidemiological studies. A physiologically-based pharmacokinetic (PBPK) model for VC was developed to support the target tissue dosimetry for the cancer risk assessment. Unlike previous models, the initial metabolism of VC was described as occurring via two saturable pathways, one representing low capacity-high affinity oxidation by CYP2E1 and the other (in the rodent) representing higher capacity-lower affinity oxidation by other isozymes of P450, producing in both cases chloroethylene oxide (CEO) and chloroacetaldehyde (CAA) as intermediate reactive products. Depletion of glutathione by reaction with CEO and CAA was also described. Animal-based risk estimates for human inhalation exposure to VC using total metabolism estimates from the PBPK model were consistent with risk estimates based on human epidemiological data, and were lower than those currently used in environmental decision-making by a factor of 80.

Keywords: Cancer; Vinyl chloride; PBPK model

* Corresponding author. Tel.: +1-318-242-5017; fax: +1-318-255-4960.
E-mail address: hclewell@icfconsulting.com (H.J. Clewell).

0048-9697/01/$ - see front matter
PII: S0048-9697(01)00730-6

1. Introduction

Vinyl chloride (VC) has been produced commercially since the 1920s (Maltoni et al., 1981). It has been used as a refrigerant, an extraction solvent, an aerosol-propellant, and even as an ingredient in drug and cosmetic products. However, when it became evident that VC was carcinogenic both in animals and in humans, these uses were discontinued; the current use of VC is limited to serving as a chemical precursor in the production of such materials as polyvinyl chloride (PVC) and copolymer resins (USEPA, 1985). Nevertheless, VC is also produced from the biodegradation of trichloroethylene by bacteria in the soil. Thus past spills of trichloroethylene may lead to current or future exposures of the public to VC in drinking water or other environmental media. The current potency estimates for VC published by the Environmental Protection Agency (EPA) do not quantitatively incorporate pharmacokinetic information on VC into the risk calculations (USEPA, 1985). The purpose of the study reported here was to re-evaluate the quantitative risk to humans of cancer from exposure to VC, using pharmacokinetics to describe the dose-response for carcinogenicity in both animals and humans.

1.1. Evidence for the carcinogenicity of VC

In 1967, Viola and colleagues initiated the first long-term bioassays using VC, in which male Wistar rats were exposed via inhalation (Viola et al., 1971). They reported a significant increase in the incidence of skin and lung carcinomas and osteochondromas. Since that time, the carcinogenicity of VC has been well established in several animal species by a number of routes of exposure. Frequently observed tumor sites in animals following VC exposure include the liver, kidney, lung, brain, mammary glands, and Zymbal glands. Of the many different tumor types which have been reported in animal bioassays of VC, three are of greater concern because they have been seen reproducibly at low concentrations (250 ppm and below): liver angiosarcoma, nephroblastoma, and mammary gland adenocarcinoma (Purchase et al., 1985). Hepatocellular carcinomas have also been occasionally observed at these low concentrations, particularly in studies of exposure to young animals (Bolt et al., 1980). Of these four low-concentration tumors, two are particularly notable in that they are rarely seen in unexposed animals: liver angiosarcoma and nephroblastoma.

Creech and Johnson (1974) reported, for the first time, an association between exposure to VC and cancer in man: three cases of liver angiosarcoma were reported in men employed in a PVC plant (Maltoni et al., 1981). Angiosarcoma of the liver is considered to be a very rare type of cancer, with only 20–30 cases per year reported in the US (Gehring et al., 1978; ATSDR, 1993). Greater than expected incidences of angiosarcoma of the liver have since been reported in a number other cohorts of workers occupationally exposed to VC (Byren et al., 1976; Infante, 1976; Fox and Collier, 1977; Jones et al., 1988; Monson et al., 1974; Pirastu et al., 1990; Rinsky et al., 1988; Teta et al., 1990; Waxweiler et al., 1976; Weber et al., 1981; Wong et al., 1986; Wu et al., 1989). Increased death due to cancer associated with VC exposure has also been reported for brain, lung, and hematopoietic systems (USEPA, 1985), as well as for other tissues, but several analyses have concluded that liver angiosarcomas show the clearest evidence for causal association and also demonstrate the highest relative risk (Purchase et al., 1985). The correspondence across species for liver hemangiosarcoma is quite striking and has made this tumor the primary focus for VC risk assessments in recent years. In particular, the correspondence across species for this tumor suggests a unique opportunity for comparing quantitative cancer risk estimates based on epidemiological data with those derived from animal bioassay data.

1.2. Previous risk assessments for VC

The EPA has performed a series of risk assessments on VC as new information has become available regarding its carcinogenic potency (USEPA 1985). In 1980 a carcinogenic potency estimate for ingestion of contaminated drinking water was determined to be 1.74×10^{-2} mg^{-1} kg

day, based on the incidence of total tumors among rats exposed by inhalation at 50–10 000 ppm, with a correction for the relationship between inhalation and oral dose levels and a cube-root body-weight-ratio correction to convert from animal to human potency. This latter correction is commonly referred to as the body-surface-area (BSA) adjustment for cross-species extrapolation. In 1984, this oral potency was revised on the basis of an oral intubation study in rats; the revised oral potency was 1.4096×10^{-1} mg^{-1} kg day, based specifically on liver angiosarcoma rather than total tumors, and again using the BSA adjustment.

In 1985, data on the total incidence of lung and liver tumors in female rats treated with diets containing VC-fortified PVC (Feron et al., 1981) was used to calculate an oral potency of 1.9 mg^{-1} kg day, which yields a unit risk of 5.4×10^{-5} μg^{-1} l. At the same time, an inhalation potency was calculated based on the studies of Maltoni et al. (1981, 1984) in which rats were exposed to concentrations of VC ranging from 1 to 30 000 ppm, 4 h day^{-1}, 5 days $week^{-1}$, for 52 weeks. The resulting inhalation potency, based on liver angiosarcoma and applying the BSA adjustment, was 2.95×10^{-1} mg^{-1} kg day, yielding a unit risk of 8.4×10^{-5} μg^{-1} m^3. The increase in the oral potency estimate from previous values was presumed to result from the availability of better tumor incidence data below the level of saturation of metabolism (USEPA, 1985). It was also noted at that time that the oral potency, expressed in milligrams per kilogram per day, was higher than the inhalation potency by roughly a factor of eight, suggesting that VC was more effective by the oral route. A subsequent study of the effect of exposure route on potency of carcinogens (Pepelko, 1991) also found that VC appeared to be more potent by the oral route when the comparison was made on the basis of mg kg^{-1} day^{-1}, and suggested that pharmacokinetic differences could underlie at least part of the discrepancy.

A pharmacokinetically-based risk assessment was proposed for VC as early as 1978 (Gehring et al., 1978). In this study it was demonstrated that the incidence of angiosarcoma correlated with amount of VC metabolized, which demonstrated Michaelis–Menten saturable kinetics, rather than with the exposure concentration of VC itself. Based on this observation and mechanistic arguments, it was proposed that daily amount metabolized should be used as the dose measure in a risk assessment for VC. Based on the limited pharmacokinetic and bioassay data available at that time, a pharmacokinetic human risk estimate for liver angiosarcoma was attempted. Their estimates of human risk at occupational exposure levels greatly overestimated the risks compared to estimates from epidemiological studies (Fox and Collier, 1977), while their predicted low-dose risks were many orders of magnitude lower than those estimated by the EPA. However, interpretation of this risk estimate is complicated by the authors' use of the probit (log probability) dose–response model rather than a linear model.

A more complete pharmacokinetic risk analysis for VC was performed (Chen and Blancato, 1989) using a physiologically-based pharmacokinetic (PBPK) description of VC kinetics and total metabolism following either oral or inhalation exposure, patterned after the PBPK model for styrene (Ramsey and Andersen, 1984). Metabolism of VC was modeled with a single saturable pathway, and the kinetic constants were estimated from measurements of whole body clearance (e.g. Filser and Bolt, 1979), although no attempt was made to validate the model against data on blood time-courses or total metabolism in rodents or humans. The model was used to calculate total metabolism of VC (representing total production of reactive metabolites) as the dose metric in a carcinogenic risk assessment for liver tumors from exposure to VC. Human inhalation potency estimates based on the internal dose metric (mg VC metabolized kg^{-1} day^{-1}) were derived from the incidence of liver tumors in rat bioassays of VC performed by Maltoni et al. (1981, 1984).

The same PBPK model was then used to estimate total metabolism for oral bioassays of VC (Maltoni et al., 1981, 1984; Feron et al., 1981). Liver tumor incidence for the oral route predicted using the PBPK dose metric (mg metabolized kg^{-1} day^{-1}) to extrapolate from the inhala-